Published in final edited form as:
Neurosci Lett. 2009 March 20; 452(3): 241–246. doi:10.1016/j.neulet.2009.01.064.

Nesfatin-1 immunoreactivity in rat brain and spinal cord autonomic nuclei

Miriam Goebel[a,*], **Andreas Stengel**[a,*], **Nils W.G. Lambrecht**[b], **Lixin Wang**[a], and **Yvette Taché**[a]

a*CURE/Digestive Diseases Research Center, Center for Neurobiology of Stress, Digestive Diseases Division, Department of Medicine, David Geffen School of Medicine, UCLA, VA Greater Los Angeles Health System, Los Angeles, California*

b*Membrane Biology Laboratory, Digestive Diseases Division, Department of Medicine, David Geffen School of Medicine, UCLA, VA Greater Los Angeles Health System, Los Angeles, California*

Abstract

Nesfatin-1 is one of the peptide products of posttranslational processing of the nucleobindin-2 (NUCB2) gene, suggested to have physiological relevance to suppress food intake and body weight gain in rats. Nesfatin-1-immunoreactive cells have been found in distinct nuclei in the rat brain related to circuitries regulating food intake. Here, we report novel yet undescribed localization of NUCB2/nesfatin-1 at the mRNA and protein level in the rat central nervous system. Immunohistochemical staining revealed the localization of NUCB2/nesfatin-1 in the piriform and insular cortex, endopiriform nucleus, nucleus accumbens, lateral septum, bed nucleus of stria terminalis, central amygdaloid nucleus, medial preoptic area, dorsal raphe nucleus, ambiguus nucleus, ventrolateral medulla and gigantocellular reticular nucleus, as well as Purkinje-cells of the cerebellum. In the spinal cord, nesfatin-1 immunoreactivity (IR) was found in both sympathetic and parasympathetic preganglionic neuronal groups and in the dorsal area X from lower thoracic to sacral segments. The immunohistochemical results were confirmed by RT-PCR in the central amygdaloid nucleus, nucleus accumbens, cerebellum and lumbar spinal cord microdissected by punch technique. The features and distributions of nesfatin-1 IR and mRNA expression in the brain and spinal cord suggest that NUCB2/nesfatin-1 could play a wider role in autonomic regulation of visceral-endocrine functions besides food intake.

Keywords

Brain; spinal cord; immunohistochemistry; mRNA expression; nucleobindin-2; rat

1. Introduction

Nesfatin-1 is a novel satiety molecule that was recently identified as a N-terminal 82 amino-acid peptide resulting from the cleavage of nucleobindin-2 (NUCB2) which can also be

Address for correspondence and reprint requests: Yvette Taché, Ph.D., Center for Neurovisceral Sciences & Women's Health, CURE Building 115, Room 117, VA Greater Los Angeles Healthcare System, 11301 Wilshire Blvd, Los Angeles, CA, 90073, USA, Tel : + 1 310 312 9275, Fax: +1 310 268 4963, E-mail: E-mail: ytache@mednet.ucla.edu.
*Authors contributed equally to this work

processed to nesfatin-2 (residues 85-163) and nesfatin-3 (residues 166-396) [14]. Intracerebroventricular (icv) injection of synthetic nesfatin-1 as well as NUCB2, unlike nesfatin-2 or nesfatin-3, induced a sustained dose-dependent reduction of food intake occurring during the dark phase in rats [14]. In addition, body weight gain was reduced upon chronic icv injection of nesfatin-1 in lean rats [14]. Potential physiological relevance of endogenous nesfatin-1 in the inhibition of food intake was suggested by the presence of nesfatin-1 detected by elution profiles of cerebrospinal fluid extracts on high-performance liquid chromatography, the stimulation of food intake induced by icv injection of a nesfatin-1 antibody [14] and the down-regulation of NUCB2 mRNA in gastric endocrine cells after 24 h fasting [20]. Recent studies have focused mainly on the co-localization of nesfatin-1 in hypothalamic and hindbrain circuitries regulating food intake such as the paraventricular nucleus (Pa), supraoptic nucleus (SO), arcuate nucleus (Arc), lateral hypothalamic area, dorsomedial hypothalamic nucleus, medullary raphe nuclei and nucleus of the solitary tract (NTS), with related co-localization with neurotransmitters/neuropeptides at these sites in rats [1,4,5,9,14]. In the present study, we revealed the expression of NUCB2/nesfatin-1 at the protein and mRNA level in rat brain extra-hypothalamic structures and in the spinal cord to round up the incomplete brain mapping of the peptide and its precursor. The present demonstration of extended NUCB2/nesfatin-1 expression in specific extra-hypothalamic brain and spinal cord areas may give impetus to unravel possible additional biological actions of the peptide.

2. Materials and Methods

Adult male Sprague-Dawley rats (Harlan, San Diego, CA, body weight of 280-350 g) were housed in groups (four animals/cage) under conditions of controlled illumination (12:12 h light/dark cycle, lights on/off: 0600 h/1800 h), and temperature (22 ± 2 °C). Animals were fed a standard rodent diet (Prolab RMH 2500; LabDiet, PMI Nutrition, Brentwood, MO) and tap water *ad libitum*. Animal care and experimental procedures followed institutional ethic guidelines and conformed to the requirements of the federal authority for animal research conduct (# 99-07-127).

Brains (n=6) and spinal cords (n=3) were harvested between 0900-1100 h from freely fed rats deeply anesthetized with intraperitoneal (ip) injection of sodium pentobarbital (70 mg/kg, Nembutal, Abbott Lab., Chicago, IL), after transcardial cannulation and perfusion (500 ml of 4% paraformaldehyde, 14% saturated picric acid in 0.1 mol phosphate buffer pH 7.2) as detailed previously [24,25]. Brains and spinal cords were post-fixed overnight in the same fixative, rinsed and cryoprotected in 10% sucrose for 24 h and snap-frozen in dry ice-cooled 2-methylbutane. Brain coronal sections (25 μm) from the bregma level 1.7 mm to the end of the medulla, according to Paxinos and Watson's atlas [15], and the spinal cord at representative segments of the cervical, thoracic, lumbar and sacral spinal cord (C7-8, T2-4, T8-9, T13-L1 and L6-S1 respectively) [15] were cut using a cryostat (Microm International GmbH, Walldorf, Germany).

Free-floating sections (every third brain section and 20-25 consecutive sections of representative spinal cord segments) were stained using the avidin-biotin-peroxidase complex (ABC) method. Endogenous peroxidase was inactivated by 0.3 % hydrogen peroxide in phosphate buffered saline (PBS) for 30 min. Sections were incubated overnight at 4 °C in rabbit polyclonal anti-nesfatin-1 antibody (1:10,000; raised against rat nesfatin-1 N-terminus (1-82); Catalog No. H-003-22, Phoenix Pharmaceuticals, Inc., Burlingame, CA), then in biotinylated goat anti-rabbit IgG (1:1,000; Jackson Immuno Research, West Grove, PA) for 1 h at room temperature (RT), followed by ABC (Vector, Vermont, CA) for 1 h at RT. Sections were developed with 3,3'-diaminobenzidine tetrahydrochloride hydrate and hydrogen peroxide (Sigma Chemical Co, St. Louis, MO) for 10 min and frequently checked with a microscope. Each step of incubation was followed by a 3 × 5 min washing step in PBS. Sections were

mounted on Fisher Super Frost Plus slides, air-dried for 24 h and completely dehydrated through a gradient of ethanol and xylene before coverslipping. Anatomical correlations were made according to landmarks given in the rat brain and spinal cord stereotaxic atlas of Paxinos and Watson [15].

The anti-nesfatin-1 antibody used was shown to stain a Western Blot band corresponding to NUCB2, which also contains the epitope (manufacturer's technical information). We also recently reported that the antibody stains rat nesfatin-1 (10kDa band) [20]. In addition, to assess the specificity of the nesfatin-1 antibody under our conditions, the same protocol was applied for immunostaining after pre-absorption of the anti-nesfatin-1 antibody. Rat nesfatin-1 (10 μg) was incubated with rabbit anti-rat nesfatin-1 at 1:10,000 in 0.3% Triton X in PBS for 2 h at room temperature followed by 22 h at 4 °C. The solution was centrifuged for 15 min at 16,000 g and the supernatant was used for staining as described above. In another control experiment we included a blocking step with normal goat serum prior to incubation with the primary antibody used at a titer of 1:20,000 instead of 1:10,000.

Nesfatin-1 immunoreactivity in the brain and spinal cord sections was examined in a light microscope (Axioscop II, Carl Zeiss, Germany) and images were acquired by a digital camera (Hamamatsu, Bridgewater, NJ) using the image acquisition system SimplePCI (Hamamatsu Corporation, Sewickley, PA). The intensity of nesfatin-1 staining was classified into two categories, namely intense or moderate relative to the established intense staining of the SO and moderate staining in the dorsal motor nucleus of the vagus [4]. The density of nesfatin-1-immunoreactive (ir) cells in each nucleus or area was determined in a field of 100 × 100 μm using a 10x objective with a grid in the ocular of the microscope in at least 5 sections, and assigned according to a scale of + to ++++ in which "+"corresponds to approximately 1-4 cells, "++" 5-10, "+++" 10-20 and "++++" more than 20 immunoreactive cells.

For expression of NUCB2 mRNA, naïve rats (n=3) were euthanized at 0900 h by decapitation and the brain and spinal cord were collected. Immediately, pieces (3×3 mm) of the lumbar part of the spinal cord and cerebellar cortex were harvested from fresh tissue whereas the forebrains were frozen on dry ice and cut in sections of 300 μm with a cryostat at -9 °C to dissect the nucleus accumbens (Acb), the Pa and the central amygdaloid nucleus (Ce) by micropunch technique according to the protocol by Mo et al. [13]. Briefly, frozen sections for each nucleus containing the region of interest (mm from bregma: Acb 2.52 to 1.8; Pa -1.56 to -1.92; Ce -2.16 to -2.52) were mounted on microscope slides. Under a stereomicroscope with reference to stained brain sections and landmarks from Paxinos and Watson's brain atlas [15], the respective areas (1×1 mm) were bilaterally dissected out with a scalpel from two sections per nucleus which were combined resulting in four punch samples/nucleus from each rat brain.

All samples were then homogenized in RNA-Bee (TEL-TEST, Friendswood, TX, USA). Total RNA was extracted and the quality and amount of final RNA yield were estimated based on ratio of absorbance at 260/280 nm by UV spectrophotometer (ND-1000; NanoDrop, Wilmington DE). Thereafter, 500 ng of total RNA of each sample was reverse-transcribed to cDNA using ThermoScript reverse transcriptase (RT) (Invitrogen, Carlsbad, CA, USA) following the manufacturer's protocol and the cDNA (1 μl) was amplified for NUCB2 directly by polymerase chain reaction (PCR) with 33 cycles at 94 °C for 40 s, 59 °C for 40 s, 72 °C for 2 min, and a final extension step at 75 °C for 5 min using the following primer pair for rat NUCB2 which has been characterized recently: sense CCA TCC AAG CAC GGT ACT GTT TTC and antisense CCA GTG TCT TGA AGG GCA TCC (373 base pairs, GenBank accession number NM 021663) [20]. Acidic ribosome protein (ARP), a house-keeping gene, served as an internal control for PCR (sense GTT GAA CAT CTC CCC CTT CTC and antisense ATG TCC TCA TCG GAT TCC TCC, 402 base pairs, GenBank accession number NM 022402).

PCR products were separated by 1% agarose gel electrophoresis and visualized with ethidium bromide. Gel images were acquired by the Kodak EDAS 290 system.

3. Results

Abundant nesfatin-1-ir neurons were observed in the ventral sites of the forebrain, including the piriform and insular cortex (Fig. 1A), endopiriform nucleus (Fig. 1A), nucleus accumbens and interstitial nucleus of the posterior limb of the anterior commissure, while the cingulate and neocortex had a lower density of nesfatin-1-ir neurons (Table 1). Nesfatin-1 labeling was mainly found in neural cytoplasm and a small number of proximal processes but not in terminals. No staining could be detected in these structures after pre-absorption of the primary antibody with the synthetic nesfatin-1 peptide (Fig. 1B) or omission of the primary antibody (data not shown). We also identified nesfatin-1-ir neurons of medium size with multipolar shape in the dorsal part of the lateral septal nucleus (Fig. 1C-D). In the bed nucleus of the stria terminalis, nesfatin-1-ir neurons with a small round profile were mainly gathered in the lateral division of the dorsal part (Fig. 1E, Table 1). In the amygdala, high density of nesfatin-1-ir neurons was found in the anterior cortical and central nucleus (Fig. 1F, Table 1). In all these sites, the intensity of nesfatin-1 staining was moderate (Table 1). To further ascertain the specificity of the immunostaining we raised the titer of the nesfatin-1 antibody to 1:20,000 and pre-treated with normal goat serum to reduce unspecific binding. Under these conditions, nesfatin-1 immunostaining was still detected in the nuclei mentioned above while the surrounding areas showed much less staining (data not shown), indicative of specific nesfatin-1 immunoreactivity.

In the hypothalamus most of the nesfatin-1-ir cells showed intense staining (Table 1). In addition to positively labeled nesfatin-1-ir cells in the SO, Pa, Arc, lateral hypothalamus and accessory neurosecretory nuclei similar to those reported recently [1,4,5,9,14], nesfatin-1-ir neurons were also detected abundantly in the medial preoptic area (Fig. 1G,Table 1). In the Pa, nesfatin-1 staining was found in the medial and lateral magnocellular Pa, whereas only scarcely detected in the parvicellular Pa (data not shown). Nesfatin-1-ir neurons were also observed in the anterior parvicellular, ventral and posterior Pa as well as dorsal cap (Fig. 1H,Table 1) and ependyma of the lateral and 3rd brain ventricles (Figs. 1C, H). In the brainstem, nesfatin-1-ir neurons showing intense staining were located in the caudal part of the central gray, nucleus O (Fig. 2B,Table 1). Neurons with moderate staining were found in all subnuclei of the dorsal raphe (ventral, dorsal and ventrolateral, Fig. 2A), external subnuclei of lateral parabrachial nucleus, A5, ventrolateral medulla (also named A1/C1, Fig. 2C), raphe magnus and gigantocellular reticular nucleus (Fig. 2E). In the medulla, nesfatin-1 immunoreactivity was localized in the ambiguus nucleus (Fig. 2D,Table 1) in addition to those reported before including the NTS and dorsal motor nucleus of the vagus [1,4,5,9,14]. The Purkinje-cells in the cerebellum were stained positively for nesfatin-1 (Fig. 2F, Table 1).

In the spinal cord, nesfatin-1-ir cells were located mainly in the autonomic preganglionic neurons in the intermediolateral cell column (IML) throughout the whole thoracic to upper lumbar (T1-L2, sympathetic, Fig. 2G) and lumbar-sacral segments (L6-S1, parasympathetic, Fig. 2H), as well as in the dorsal part of area X of the lower thoracic-upper lumbar (T13-L1) and lumbar-sacral segments (L6-S1) (Fig. 2I, Table 1). Occasionally, a few of nesfatin-1-ir neurons were observed in laminae III, IV and IX, and the dorsolateral fascicular nucleus. There was no nesfatin-1 labeling in the cervical spinal cord. The ependyma of the central canal in the spinal cord also displayed intense staining (Fig. 2I).

Using the primers designed to target the rat NUCB2 gene, the expected size of 373 base pair PCR product for NUCB2 was detected in the central amygdaloid nucleus, nucleus accumbens,

cerebellar cortex, lumbar spinal cord and Pa (positive control) harvested by microdissection (Fig. 3).

4. Discussion

Immunohistochemical localization of nesfatin-1 in the rat brain has been extensively described in hypothalamic and brainstem nuclei namely the Pa, SO, Arc, lateral hypothalamic area, dorsomedial hypothalamic nucleus, Edinger-Westphal nucleus, medullary raphe nuclei and dorsal vagal complex [1,4,5,9,14]. In the present study, consistent with previous reports, we also found a similar pattern of nesfatin-1 staining in these brain nuclei. However in addition, we revealed a more extensive distribution of nesfatin-1 staining in specific forebrain and hindbrain nuclei as well as the spinal cord, which have not been previously identified. In particular, immunolabeling was detected in the piriform and insular cortex, endopiriform nucleus, lateral septum, central amygdaloid nucleus, dorsal raphe nuclei, ambiguus nucleus, ventrolateral medulla and cerebellum. Furthermore, we observed the presence of nesfatin-1 immunoreactivity in preganglionic sympathetic and parasympathetic neurons of the thoracic, lumbar and sacral spinal cord. Several established measures were taken to ascertain the specificity of the commercially available nesfatin-1 antiserum used in the present study [18]. In particular, nesfatin-1 immunolabeling in forebrain, hindbrain and spinal cord was abolished when using antibody pre-absorbed with synthetic nesfatin-1 peptide. In addition, we showed site specificity of the spinal immunostaining with no nesfatin-1 labeling at the cervical level. Besides nesfatin-1, the antibody used also recognizes the full length NUCB2, but does not cross-react with other neuropeptides [1]. Therefore, the present expression pattern is likely to reflect nesfatin-1/NUCB2 immunoreactivity. This is supported by a recent report showing a similar hypothalamic and brainstem distribution by immunohistochemistry using antisera raised against rat nesfatin-1, -2 or -3 and *in situ* labeling using NUCB2 mRNA probe [4]. Likewise, we found that NUCB2 mRNA expression could be detected in the cerebral cortex, central amygdaloid nucleus, nucleus accumbens and lumbar spinal cord consistent with nesfatin-1 immunolabeling at these specific brain and spinal sites. As reported previously [4, 14] the NUCB2 mRNA signal could be detected in the Pa which served as a positive control. However, it cannot be ruled out that there is a brain area-specific processing of NUCB2 leading selectively to nesfatin-1 protein expression in these newly described sites. We recently showed differential occurrence of different molecular weight proteins in soluble and membrane fractions of the pituitary gland, stomach and pancreas by Western blot analysis with anti-rat nesfatin-1 antibody [20].

Nesfatin-1 staining was located mainly in neuronal cell bodies, but not in terminals consistent with previous observations, showing the lack of nesfatin-1 immunolabeling in varicosities or terminal-like structures [1,4]. The fact that nesfatin-1 immunoreactivity is not readily detectable in nerve fibers suggests that nesfatin-1 and/or NUCB2 may function as an intracellular modulator rather than as transmitter or neuronal peptide. Colchicine treatment, commonly used in immunohistochemistry to interrupt axonal transport and to retain accumulation of secreted molecules in neuronal cell bodies, did not increase and rather decreased nesfatin-1 immunoreactivity in lateral hypothalamic cells [4]. It is unlikely that the local nesfatin-1 concentration in the fibers was below the threshold for immunohistochemical detection as neuropeptides and transmitters are immunohistochemically easier to detect in terminals than in the cytoplasm. The lack of nesfatin-1-ir neuronal terminals is not conflicting with the finding that nesfatin-1 was found as a secreted fragment in the cerebrospinal fluid [14], as dendrites and soma have been shown to release cellular contents [2,10]. Moreover, the nesfatin-1 precursor NUCB2 possesses functional domains of a signal peptide and a putative nuclear targeting signal [8,22], indicating that NUCB2/nesfatin-1 may function as a cellular signal.

While the previously reported distribution pattern of nesfatin-1 was centered on interconnected regions implicated in orchestrating feeding behavior and neuroendocrine regulation [1,4,5,9, 14], the present data expand the characterization of NUCB2/nesfatin-1 distribution within brain and spinal autonomic regulatory centers and forebrain structures modulating autonomic outflow to the viscera and autonomic response to emotion and pain. This is supported by the expression of nesfatin-1 immunoreactivity at supraspinal and spinal sites involved in sympathetic and parasympathetic regulation of the cardiovascular and gastrointestinal function such as the dorsal cap of the Pa, ventrolateral medulla, ambiguus nucleus and intermediolateral cell column of the spinal cord [11,21]. Nesfatin-1 was also identified in the limbic system, namely the central amygdaloid nucleus and bed nucleus of the stria terminalis that provide input to structures important in arousal and anxiety and associated autonomic changes [17]. Of interest was the recent demonstration that nesfatin-1 induced anxiety and fear-related behavior [12]. Detection of nesfatin-1 labeling within the parabrachial area, gigantocellular reticular nucleus and nucleus raphe magnus may also suggest a role in pain processing since the parabrachial nucleus participates in the genesis of the emotional components of pain and related autonomic adaptation [6] and the raphe magnus is part of the descending pain control system [23]. The presence of nesfatin-1 in the lateral septum, cortical areas and nucleus accumbens is indicative that nesfatin-1 may be in position to influence regulatory processes related to mood and motivation [7,19].

The detailed distribution of nesfatin-1-ir neurons in paraventricular subnuclei which are well established to express different neuroendocrine peptides, neurotransmitters and receptors and are thus implicated in different functions [3] further strengthens the possible broader physiological role of NUCB2/nesfatin-1 in the regulation of fluid homeostasis, cardiovascular system and in stress response. Indeed, a recent study showed that nesfatin-1 directly influences the excitability of nearly all subtypes of paraventricular neurons irrespective of being magnocellular, preautonomic or neuroendocrine parvicellular neurons as assessed in electrophysiological patch clamp recordings [16].

In summary, the immunohistochemical distribution of NUCB2/nesfatin-1 in cell bodies in brain autonomic regulatory centers and preganglionic visceral motor neurons in the brain and the spinal cord along with other forebrain nuclei involved in pain coding and cognitive behavior supports the assumption that nesfatin-1/NUCB2 may be, in addition to regulating food intake, involved in the autonomic integration of cardiovascular, emotional and neuroendocrine mechanisms.

Acknowledgements

This work was supported by German Research Foundation grant GO 1718/1-1 (M.G.), grant STE 1765/1-1 (A.S.) and the VA Research Career Scientist Award, Department of Veterans Affairs Merit Award (Y.T.), NIHDK 33061 (Y.T.) and Center grant DK-41301 (Animal Core, Y.T.). We are grateful to Mrs. Honghui Liang for her excellent technical support.

References

1. Brailoiu GC, Dun SL, Brailoiu E, Inan S, Yang J, Chang JK, Dun NJ. Nesfatin-1: distribution and interaction with a G protein-coupled receptor in the rat brain. Endocrinology 2007;148:5088–5094. [PubMed: 17627999]
2. Bustos G, Abarca J, Campusano J, Bustos V, Noriega V, Aliaga E. Functional interactions between somatodendritic dopamine release, glutamate receptors and brain-derived neurotrophic factor expression in mesencephalic structures of the brain. Brain Res Brain Res Rev 2004;47:126–144. [PubMed: 15572168]

3. Ferguson AV, Latchford KJ, Samson WK. The paraventricular nucleus of the hypothalamus - a potential target for integrative treatment of autonomic dysfunction. Expert Opin Ther Targets 2008;12:717–727. [PubMed: 18479218]
4. Foo K, Brismar H, Broberger C. Distribution and neuropeptide coexistence of nucleobindin-2 mRNA/nesfatin-like immunoreactivity in the rat CNS. Neuroscience 2008;156:563–579. [PubMed: 18761059]
5. Fort P, Salvert D, Hanriot L, Jego S, Shimizu H, Hashimoto K, Mori M, Luppi PH. The satiety molecule nesfatin-1 is co-expressed with melanin concentrating hormone in tuberal hypothalamic neurons of the rat. Neuroscience 2008;155:174–181. [PubMed: 18573315]
6. Gauriau C, Bernard JF. Pain pathways and parabrachial circuits in the rat. Exp Physiol 2002;87:251–258. [PubMed: 11856971]
7. Goto Y, Grace AA. Limbic and cortical information processing in the nucleus accumbens. Trends Neurosci 2008;31:552–558. [PubMed: 18786735]
8. Karabinos A, Bhattacharya D, Kratzin HD, Hilschmann N. Origin of the NEFA and Nuc signal sequences. J Mol Evol 1998;46:327–333. [PubMed: 9493357]
9. Kohno D, Nakata M, Maejima Y, Shimizu H, Sedbazar U, Yoshida N, Dezaki K, Onaka T, Mori M, Yada T. Nesfatin-1 neurons in paraventricular and supraoptic nuclei of the rat hypothalamus coexpress oxytocin and vasopressin and are activated by refeeding. Endocrinology 2008;149:1295–1301. [PubMed: 18048495]
10. Landgraf R, Neumann ID. Vasopressin and oxytocin release within the brain: a dynamic concept of multiple and variable modes of neuropeptide communication. Front Neuroendocrinol 2004;25:150–176. [PubMed: 15589267]
11. Lovick TA. The medullary raphe nuclei: a system for integration and gain control in autonomic and somatomotor responsiveness? Exp Physiol 1997;82:31–41. [PubMed: 9023504]
12. Merali Z, Cayer C, Kent P, Anisman H. Nesfatin-1 increases anxiety- and fear-related behaviors in the rat. Psychopharmacology 2008;201:115–123. [PubMed: 18670764]
13. Mo B, Callegari E, Telefont M, Renner KJ. Proteomic analysis of the ventromedial nucleus of the hypothalamus (pars lateralis) in the female rat. Proteomics 2006;6:6066–6074. [PubMed: 17051637]
14. Oh IS, Shimizu H, Satoh T, Okada S, Adachi S, Inoue K, Eguchi H, Yamamoto M, Imaki T, Hashimoto K, Tsuchiya T, Monden T, Horiguchi K, Yamada M, Mori M. Identification of nesfatin-1 as a satiety molecule in the hypothalamus. Nature 2006;443:709–712. [PubMed: 17036007]
15. Paxinos, G.; Watson, C. The Rat Brain in Stereotaxic Coordinates. Academic Press; San Diego: 2007.
16. Price CJ, Hoyda TD, Samson WK, Ferguson AV. Nesfatin-1 influences the excitability of paraventricular nucleus neurones. J Neuroendocrinol 2008;20:245–250. [PubMed: 18088358]
17. Saper, CB. The rat nervous system. Academic Press; San Diego: 2005. Central autonomic system; p. 107-128.
18. Saper CB. An open letter to our readers on the use of antibodies. J Comp Neurol 2005;493:477–478. [PubMed: 16304632]
19. Sheehan TP, Chambers RA, Russell DS. Regulation of affect by the lateral septum: implications for neuropsychiatry. Brain Res Brain Res Rev 2004;46:71–117. [PubMed: 15297155]
20. Stengel A, Goebel M, Yakubov I, Wang L, Witcher D, Coskun T, Taché Y, Sachs G, Lambrecht NW. Identification and characterization of nesfatin-1 immunoreactivity in endocrine cell types of the rat gastric oxyntic mucosa. Endocrinology 2009;150:232–238. [PubMed: 18818289]
21. Taché Y, Yang H, Kaneko H. Caudal raphe-dorsal vagal complex peptidergic projections: role in gastric vagal control. Peptides 1995;16:431–435. [PubMed: 7544464]
22. Valencia CA, Cotten SW, Duan J, Liu R. Modulation of nucleobindin-1 and nucleobindin-2 by caspases. FEBS Lett 2008;582:286–290. [PubMed: 18154733]
23. Vanegas H, Schaible HG. Descending control of persistent pain: inhibitory or facilitatory? Brain Res Brain Res Rev 2004;46:295–309. [PubMed: 15571771]
24. Wang L, Martinez V, Barrachina MD, Taché Y. Fos expression in the brain induced by peripheral injection of CCK or leptin plus CCK in fasted lean mice. Brain Res 1998;791:157–166. [PubMed: 9593872]

25. Wang L, Saint-Pierre DH, Taché Y. Peripheral ghrelin selectively increases Fos expression in neuropeptide Y - synthesizing neurons in mouse hypothalamic arcuate nucleus. Neurosci Lett 2002;325:47–51. [PubMed: 12023064]

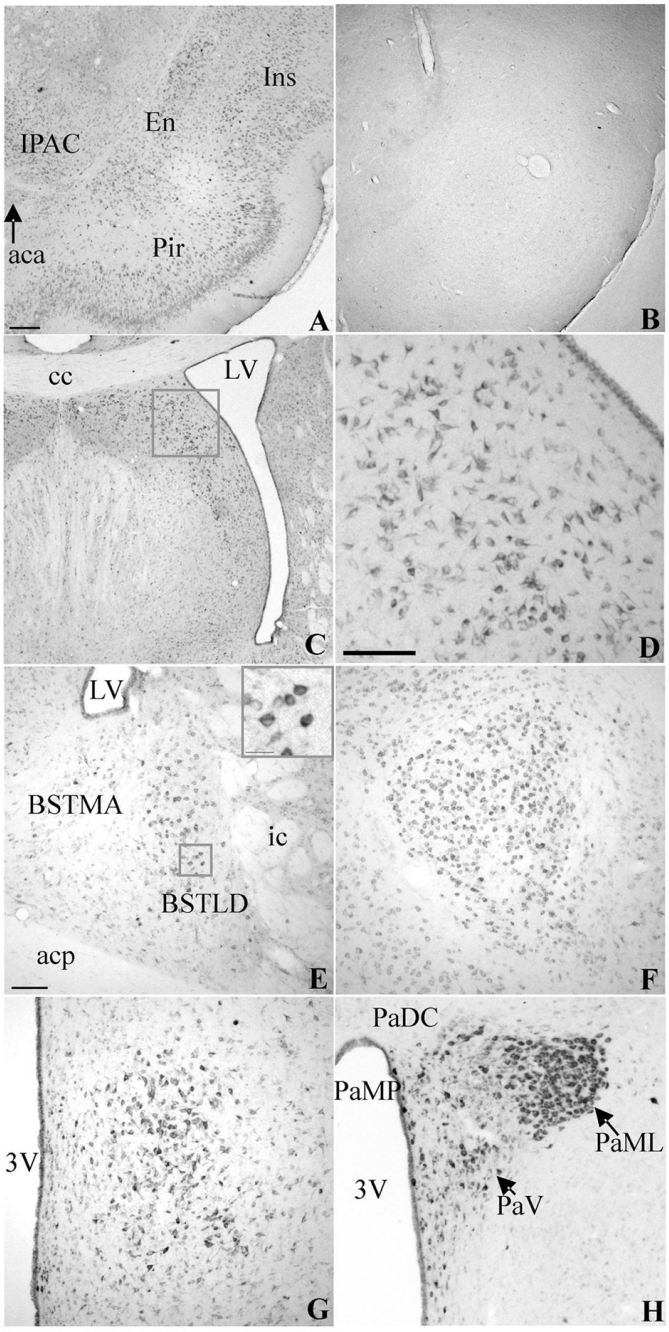

Figure 1.

Representative microphotographs of nesfatin-1 immunoreactive cells in the forebrain and hypothalamus in naïve rats. (A) Basolateral forebrain structure including piriform (Pir) and insular cortex (Ins), endopiriform nucleus (En) and interstitial nucleus of the posterior limb of the anterior commissure (IPAC). (B) No staining can be detected following pre-absorption of the antibody with nesfatin-1 peptide in the same area as in A. (C) Septum. (D) Nesfatin-1-ir neurons of the dorsal part of the lateral septal nucleus with higher magnification of the framed area in panel C. (E) Lateral division in the dorsal part of the bed nucleus of the stria terminalis (BSTLD). The insert illustrates the small round profile of the neurons. (F) Central amygdaloid nucleus. (G) Medial preoptic area. (H) Medial parvicellular (PaMP), magnocellular lateral

(PaML), ventral (PaV) Pa and dorsal cap (PaDC). Scale bars: A-C: 200 μm, D-H: 100 μm, insert in E: 25 μm. Other abbreviations: 3V: third ventricle; aca: anterior commissure, anterior part; acp: anterior commissure, posterior part; cc: corpus callosum; ic: internal capsule; LV: lateral ventricle; BSTMA: bed nucleus of the stria terminalis, medial division, anterior part.

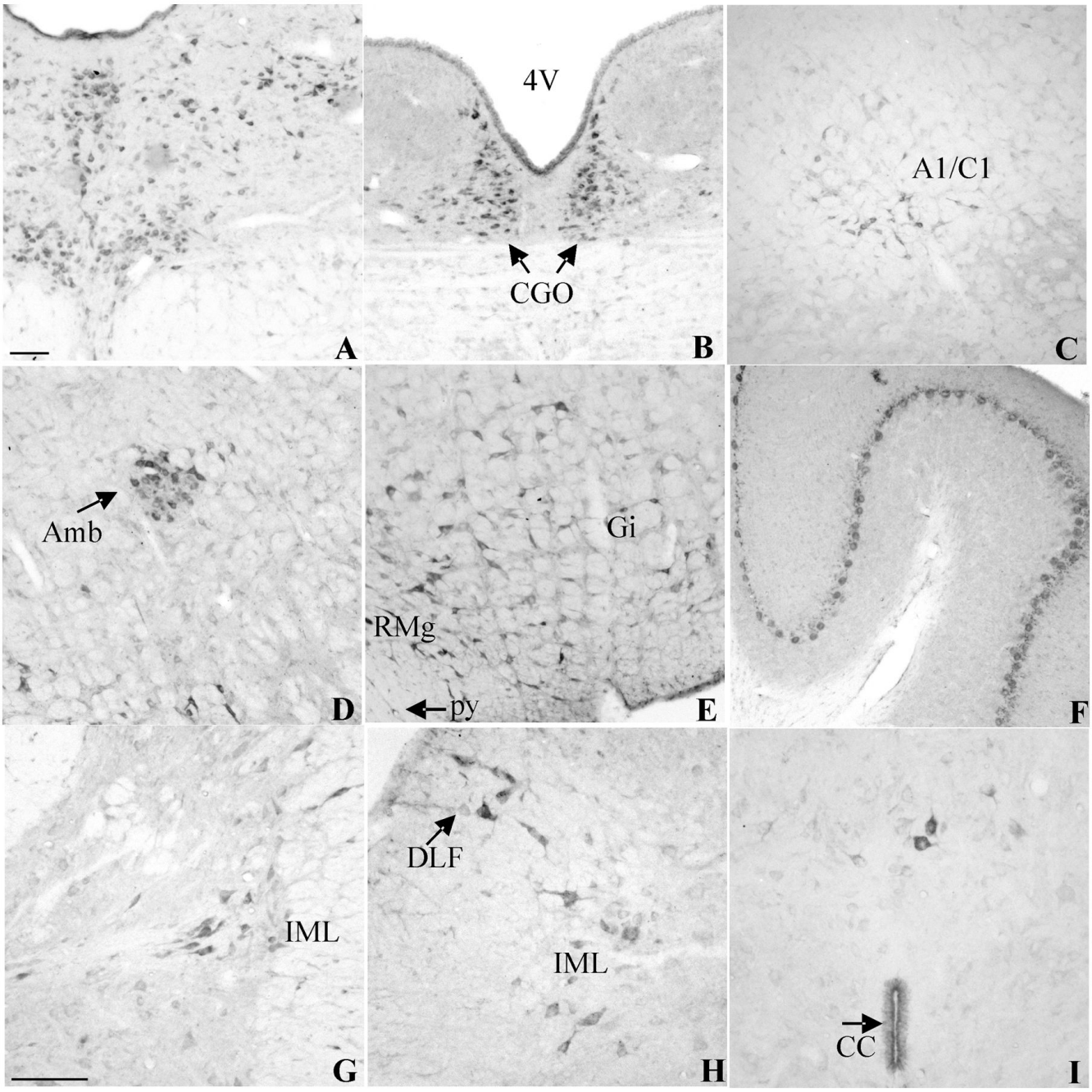

Figure 2.

Nesfatin-1 immunoreactive cells in the midbrain, pons, medulla, cerebellum and spinal cord in naïve rats. (A) Dorsal raphe nucleus. (B) Central gray, nucleus O (CGO). (C) A1/C1. (D) Ambiguus nucleus (Amb). (E) Gigantocellular reticular nucleus (Gi). (F) Purkinje-cells in the cerebellum. (G) Intermediolateral cell column (IML) of the spinal cord at T2–T4. (H) IML at S1. (I) Dorsal area X at S1. Scale bars: A-I: 100 μm. Other abbreviations: 4V: fourth ventricle; CC: central canal; py: pyramid tract; RMg: raphe magnus nucleus.

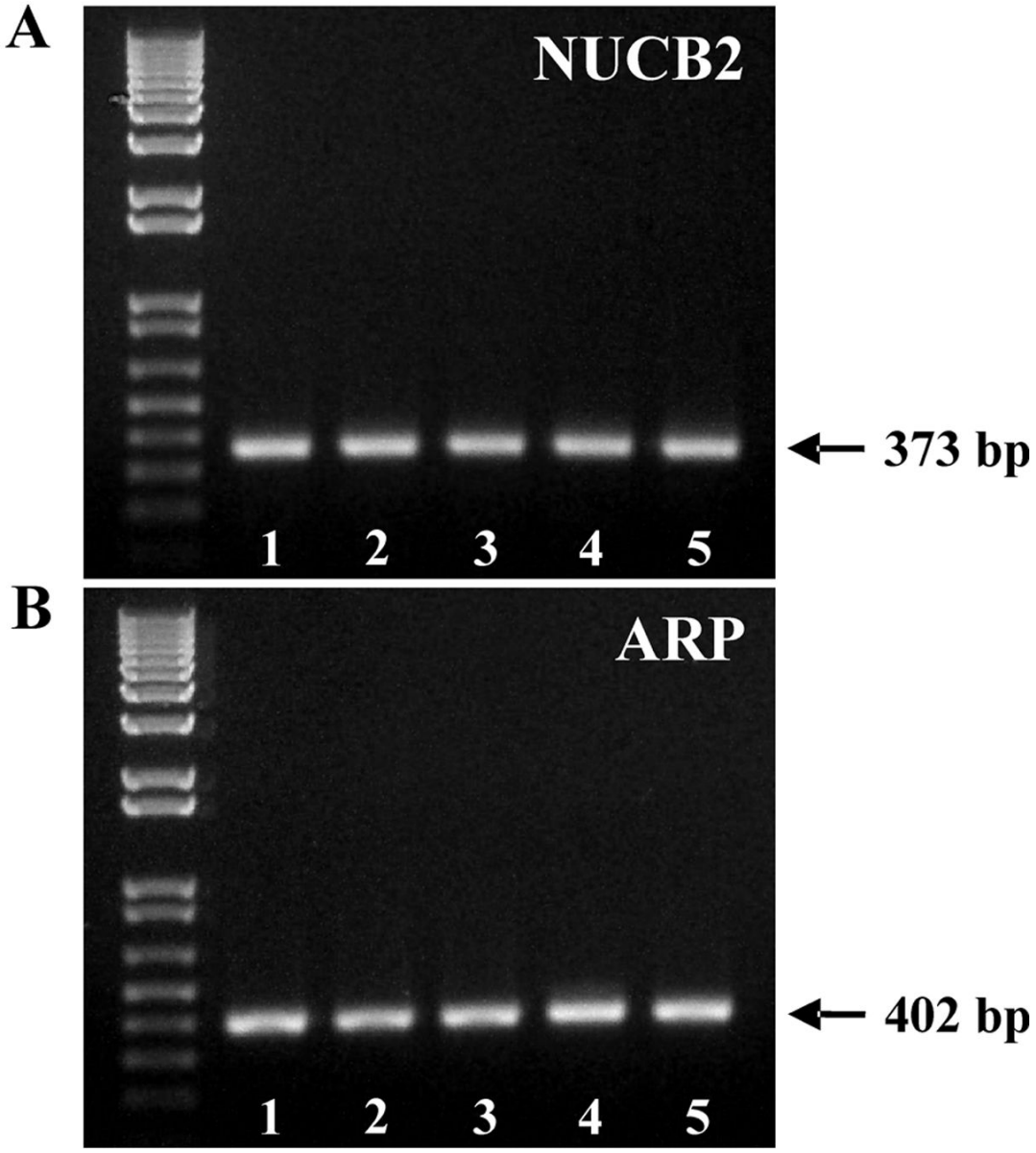

Figure 3.

Nucleobindin-2 (NUCB2) gene expression in representative areas of the brain and spinal cord in naïve rats. Gel images of RT-PCR for NUCB2 (A) and house-keeping gene ARP (B) in the central amygdaloid nucleus (lane 1), nucleus accumbens (lane 2), cerebellar cortex (lane 3), lumbar spinal cord (lane 4) and Pa (lane 5). The predicted base pair (bp) PCR products for NUCB2 (373 bp) and ARP (402 bp) were observed in all areas.

Table 1

Rat brain nuclei with nesfatin-1 immunoreactivity. Density: "+" approximately 1-4 cells, "++" 5-10, "+++" 10-20 and "++++" > 20 immunoreactive cells in a 100 × 100 μm area of an ocular grid when the objective was 10x. Intensity: M: moderate; I: intensive (see representative nuclei in Fig. 1 and 2).

	Brain structure	Density	Intensity
Forebrain	accumbens nucleus	+++	M
	piriform cortex	++	M
	insular cortex	++	M
	cingulate cortex	+	M
	endopiriform nucleus	++	M
	lateral septum	++	M
	bed nucleus of the stria terminalis lateral division of the dorsal part	+++	M
	interstitial nucleus of the posterior limb of the anterior commissure	+++	M
	other cortical areas	+	M
	anterior cortical amygdaloid nucleus	++	M
	central amygdaloid nucleus	+++	M
Hypothalamus	medial preoptic area	++	I
	paraventricular nucleus		
	parvicellular anterior	++	I
	parvicellular medial	+	I
	ventral	+ ~ ++	I
	magnocellular medial	+++	I
	magnocellular lateral	++++	I
	posterior	+ ~ ++	I
Midbrain	dorsal raphe nucleus	+++	M
Pons	external subnucleus of lateral parabrachial nucleus	+	M
	central gray, nucleus O	++ ~ +++	I
	A5	+	M
Medulla	gigantocellular reticular nucleus	+	M
	raphe magnus nucleus	++	M
	ambiguus nucleus	++	M
	A1/C1	++	M
Cerebellum	Purkinje-cells	+++	M
Spinal cord	intermediolateral cell column	++	M
	dorsal area X	+	M